A GES mass flow observer for compression systems: Design and Experiments

Bjørnar Bøhagen
Department of Engineering Cubernetics
Norwegian University of Science and Technology
N-7491 Trondheim
bjornar.bohagen@itk.ntnu.no

Olav Stene
Statoil ASA
N-4035 Stavanger
olste@statoil.com

Jan Tommy Gravdahl
Department of Engineering Cubernetics
Norwegian University of Science and Technology
N-7491 Trondheim
tommy.gravdahl@itk.ntnu.no

***Abstract*— In this paper we present a novel globally exponentially stable (GES) mass flow observer for compression systems. A nonlinear separation principle for a class of controllers for the compression system is shown, allowing a control law and the proposed observer to be tuned separately. The results are supported by simulations and experiments.**

I. BACKGROUND

Towards low mass flows, the stable operating region of centrifugal compressors is bounded due to the occurrence of surge. Surge is characterized by oscillations in the pressure rise and mass flow. These oscillation can cause severe damage to the machine due to vibrations and high thermal loading resulting from lowered efficiency. Surge is an unstable operation mode of the compressor and the stability boundary in the compressor map is called the surge line. Traditionally, surge has been avoided using surge avoidance schemes. Such schemes use various measurements in order to keep the operating point of the compressor away from the region where surge occurs. Typically, a surge control line is drawn at a distance away from the surge line, and the surge avoidance scheme ensures that the operating point does not cross this line. This method restricts the operating range of the machine, and efficiency is limited. Usually a recycle line around the compressor is used as actuation.

Active surge control is fundamentally different from surge avoidance. In an active surge control scheme the open loop unstable phenomena is sought stabilized rather than avoided. Thus the operating regime of the machine is enlarged. Active surge control of compressors was first introduced by [1], and since then a number of results have been published. Different actuators have been used and examples include recycle, bleed and throttle valves, gas injection, variable guide vanes, drive torque and a number of others. For an overview, consult [2] and [3].

Several active surge control algorithms rely on feedback from mass flow. It is however well known that real time measurements of mass flow is both expensive and hampered with high noise levels. This motivates the work of designing surge controllers using mass flow observers, where the mass flow estimate is used in the control algorithms rather than mass flow measurement. In [4] a mass flow observer was proposed, and a separation principle allowing the controller and the observer to be tuned separately was shown. The observer algorithm from [4] uses a model for the compressor characteristics. The compressor characteristics is in some cases or regions poorly known. This motivated the work of designing a mass flow observer whose observer algorithm was independent of the compressor characteristics.

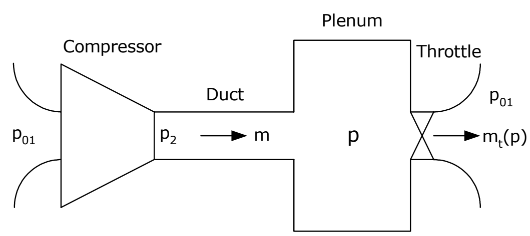

Fig. 1. Compression system

II. MODEL

A classical result in the field of compressor surge modeling is the model of Greitzer [5] who modelled a basic compression system consisting of a compressor, a plenum volume, in-between ducting and a throttle valve as shown in Fig. 1. The authors of [6] extend the Greizer-model to include rotational speed as a state in the model. A similar model was derived in [7], using an approach based on energy analysis. In this paper the model given in [2] will be employed. The model is derived by calculating the mass balance of the plenum volume, integrating the one dimensional Euler equation (the momentum balance) over the length of the duct and calculating the torque balance of the rotating shaft. The model is written

$$\dot{p} = \frac{a_{01}^2}{V_p}\left(m - m_t\left(p\right)\right) \tag{1}$$

$$\dot{m} = \frac{A_1}{L_c}\left(p_2\left(m,\omega\right) - p\right) \tag{2}$$

$$\dot{\omega} = \frac{1}{J}\left(\tau_d - \tau_c\left(m,\omega\right)\right) \tag{3}$$

where p is the plenum pressure, m is the compressor mass flow, ω is the rotational speed of the shaft driving the compressor, $m_t\left(p\right)$ is the mass flow through the throttle valve, $p_2\left(m,\omega\right)$ is the pressure at the outlet of the compressor, τ_d is the torque driving the compressor, $\tau_c\left(m,\omega\right)$ is the compressor load torque, a_{01} is the sonic velocity at ambient conditions, V_p is the plenum volume, A_1 is the duct throughflow area, L_c

0-7803-8335-4/04/$17.00 ©2004 AACC

is the length of the duct and J is the inertia of rotating parts. The mass flow through the throttle and the compressor torque are given by

$$m_t(p) = k_t\sqrt{p-p_{01}} \quad (4)$$
$$\tau_c(m,\omega) = \sigma r_2^2 |m| \omega \quad (5)$$

where $k_t > 0$ is a parameter proportional to the throttle opening, p_{01} is the ambient pressure, σ is the slip factor and r_2 is the impeller diameter. The mass flow dynamics (2) is often expressed using the compressor characteristics $\psi(m,\omega)$, where $p_2(m,\omega) = \psi(m,\omega)p_{01}$. For a detailed derivation of the model, consult [2].

III. Observer

Due to the practical difficulties of implementing a controller dependent on a mass flow measurement, a GES observer for the mass flow through the compressor is proposed. The estimated variable will be denoted by $\hat{(\cdot)}$ and the observer error will be denoted by $\tilde{(\cdot)}$.

Definition 1 (Observer error):

$$\tilde{m} = m - \hat{m}$$

The observer uses measurements of the plenum pressure and the pressure at the outlet of the compressor. In addition to these measurements the observer will make use of possible control inputs appearing in the pressure dynamics (2). Let the measured pressure at the outlet of the compressor be denoted p_2 and any control input appearing in the mass flow dynamics be denoted u. First, the observer is analyzed disregarding uncertainty in the measurements. Then the effect of uncertainty in the measurements is analyzed.

A. Disregarding uncertainty in the measurements

Assumption 1: $p > p_{01}\ \forall t \geq t_0$

Proposition 1: Under Assumption 1 the observer

$$\dot{z} = \frac{A_1}{L_c}(p_2 - p - u) - k_{\tilde{m}}\hat{m} + k_{\tilde{m}} m_t(p) \quad (6)$$
$$\hat{m} = z + k_{\tilde{m}}\frac{V_p}{a_{01}^2}p \quad (7)$$

where $k_{\tilde{m}} > 0$ is the observer gain, makes the equilibrium $\tilde{m} = 0$ GES.

Assumption 1 guarantees that $m_t(p) \in \mathbb{R}\ \forall t \geq t_0$, which guarantees that $\dot{z} \in \mathbb{R}\ \forall t \geq t_0$.

Proof: Using (7), (6) and (1), the observer dynamics is found as

$$\begin{aligned}\dot{\hat{m}} &= \frac{A_1}{L_c}(p_2 - p - u) - k_{\tilde{m}}\hat{m} + k_{\tilde{m}} m_t(p) \\ &\quad + k_{\tilde{m}}\frac{V_p}{a_{01}^2}\left(\frac{a_{01}^2}{V_p}(m - m_t(p))\right) \\ &= \frac{A_1}{L_c}(p_2 - p - u) + k_{\tilde{m}}\tilde{m} \quad (8)\end{aligned}$$

and by using Definition 1, (8) and (2) the observer error dynamics is found as

$$\begin{aligned}\dot{\tilde{m}} &= \frac{A_1}{L_c}(p_2(m,\omega) - p - u) - \frac{A_1}{L_c}(p_2 - p - u) - k_{\tilde{m}}\tilde{m} \\ &= -k_{\tilde{m}}\tilde{m} \quad (9)\end{aligned}$$

Consider the Lyapunov function candidate

$$V(\tilde{m}) = \frac{1}{2}\tilde{m}^2 \quad (10)$$

The time derivative of V along the trajectories of (9) is found as

$$\dot{V}(\tilde{m}) = -k_{\tilde{m}}\tilde{m}^2 \quad (11)$$

Equations (10)-(11) implies that the function $V(\tilde{m})$ is a Lyapunov function for the estimated mass flow error satisfying globally exponential stability of the equilibrium $\tilde{m} = 0$. ■

Remark 1: The solution $\tilde{m}(t)$ is bounded by $|\tilde{m}(t)| \leq |\tilde{m}(t_0)| e^{-k_{\tilde{m}}(t-t_0)}$, which shows that the rate of convergence is given by the magnitude of $k_{\tilde{m}}$.

B. Including uncertainty in the measurements

The observer from the previous section will now be analyzed when taking uncertainty in the measurements into account.

Definition 2 (Measured variables):

$$p_m = p + \delta_p(t)$$
$$p_{2_m} = p_2 + \delta_{p_2}(t)$$

where p_m and p_{2_m} are measured signals and $\delta_p(t)$, $\delta_{p_2}(t)$ and $\dot{\delta}_p(t)$ are bounded and piecewise continuous signals.

By including uncertainty in the measurements used by the observer (6)-(7), the implementation is given by

$$\dot{z} = \frac{A_1}{L_c}(p_{2m} - p_m - u) - k_{\tilde{m}}\hat{m} + k_{\tilde{m}} m_t(p_m) \quad (12)$$
$$\hat{m} = z + k_{\tilde{m}}\frac{V_p}{a_{01}^2}p_m \quad (13)$$

Assumption 2: $p > p_{01} - \delta_p(t)\ \forall t \geq t_0$

Proposition 2: Under Assumption 2 the observer (12)-(13), where $k_{\tilde{m}} > 0$ is the observer gain, makes $\tilde{m}(t)$ globally uniformly ultimately bounded with the ultimate bound

$$b = \frac{\delta}{k_{\tilde{m}}\theta}$$

where $\theta \in \langle 0, 1\rangle$ and δ is given by

$$\delta = \sup\left|\frac{A_1}{L_c}(\delta_{p_2}(t) - \delta_p(t)) + k_{\tilde{m}}\delta_{m_t}(t) + k_{\tilde{m}}\frac{V_p}{a_{01}^2}\dot{\delta}_p(t)\right|$$

Moreover, $\tilde{m}(t)$ converges exponentially to the set $\{\tilde{m} \in \mathbb{R} \mid |\tilde{m}| \leq b\}$ in finite time.

Proof: Using (13), (12) and (1) the observer dynamics is found as

$$\begin{aligned}\dot{\hat{m}} &= \frac{A_1}{L_c}\left(p_{2m}-p_m-u\right)-k_{\tilde{m}}\hat{m}+k_{\tilde{m}}m_t\left(p_m\right)\\ &\quad +k_{\tilde{m}}\frac{V_p}{a_{01}^2}\left(\dot{p}+\dot{\delta}_p\left(t\right)\right)\\ &= \frac{A_1}{L_c}\left(p_2-p-u\right)+k_{\tilde{m}}\tilde{m}+k_{\tilde{m}}\left(m_t\left(p_m\right)-m_t\left(p\right)\right)\\ &\quad +\frac{A_1}{L_c}\left(\delta_{p_2}\left(t\right)-\delta_p\left(t\right)\right)+k_{\tilde{m}}\frac{V_p}{a_{01}^2}\dot{\delta}_p\left(t\right) \qquad (14)\end{aligned}$$

The term $m_t\left(p_m\right)$ may be rewritten as

$$m_t\left(p_m\right)=m_t\left(p\right)+\delta_{m_t}\left(t\right) \qquad (15)$$

where $\delta_{m_t}\left(t\right)$ is bounded due to the upper bound on $\delta_p\left(t\right)$ and the lower bound on p imposed by Assumption 2. Using (15) the observer dynamics (14) may now be written as

$$\begin{aligned}\dot{\hat{m}} &= \frac{A_1}{L_c}\left(p_2-p-u\right)+k_{\tilde{m}}\tilde{m}\\ &\quad +\frac{A_1}{L_c}\left(\delta_{p_2}\left(t\right)-\delta_p\left(t\right)\right)+k_{\tilde{m}}\frac{V_p}{a_{01}^2}\dot{\delta}_p\left(t\right)+k_{\tilde{m}}\delta_{m_t}\left(t\right)\\ &= \frac{A_1}{L_c}\left(p_2-p-u\right)+k_{\tilde{m}}\tilde{m}+\delta\left(t\right) \qquad (16)\end{aligned}$$

where

$$\delta\left(t\right)=\frac{A_1}{L_c}\left(\delta_{p_2}\left(t\right)-\delta_p\left(t\right)\right)+k_{\tilde{m}}\delta_{m_t}\left(t\right)+k_{\tilde{m}}\frac{V_p}{a_{01}^2}\dot{\delta}_p\left(t\right) \quad (17)$$

is bounded by Definition 2 And Assumption 2. The observer error dynamics is found by using Definition 1, (16) and (2)

$$\begin{aligned}\dot{\tilde{m}} &= \frac{A_1}{L_c}\left(p_2\left(m,\omega\right)-p-u\right)\\ &\quad -\frac{A_1}{L_c}\left(p_2-p-u\right)-k_{\tilde{m}}\tilde{m}-\delta\left(t\right)\\ &= -k_{\tilde{m}}\tilde{m}-\delta\left(t\right) \qquad (18)\end{aligned}$$

Using (18), [8, Lemma 9.2] and (9)-(11)it is concluded that

$$\begin{aligned}\left|\tilde{m}\left(t\right)\right| &\leq e^{-k_{\tilde{m}}(1-\theta)(t-t_0)}\left|\tilde{m}_0\right| \quad \forall t_0\leq t\leq t_0+T \quad (19)\\ \left|\tilde{m}\left(t\right)\right| &\leq \frac{\delta}{k_{\tilde{m}}\theta} \quad \forall t\geq t_0+T \quad (20)\end{aligned}$$

for some finite T, where $\delta=\sup\left|\delta\left(t\right)\right|$ and $\theta\in\langle 0,1\rangle$. ■

Remark 2: From (19) it can be seen that the rate of convergence for $\tilde{m}\left(t\right)$ to the set $\left\{\tilde{m}\in\mathbb{R}|\left|\tilde{m}\right|\leq b\right\}$ is given by the magnitude of $k_{\tilde{m}}$.

Remark 3: From (20) and (17) it can be seen the ultimate bound on $\tilde{m}\left(t\right)$ is upper bounded by

$$b=\frac{\sup\left|\frac{A_1}{k_{\tilde{m}}L_c}\left(\delta_{p_2}\left(t\right)-\delta_p\left(t\right)\right)+\delta_{m_t}\left(t\right)+\frac{V_p}{a_{01}^2}\dot{\delta}_p\left(t\right)\right|}{\theta}$$

where it can be seen that a large $k_{\tilde{m}}$ suppresses the effect of the uncertainty $\left(\delta_{p_2}\left(t\right)-\delta_p\left(t\right)\right)$ on b, whereas it does not influence on the effects from the uncertainties $\delta_{m_t}\left(t\right)$ and $\dot{\delta}_p\left(t\right)$.

IV. A SEPARATION PRINCIPLE

In this section the stability of the overall system is analyzed when the estimated mass flow is used in a feedback control law. It will be shown that a controller, which is assumed to turn the closed loop system exponentially stable, and the mass flow observer from Proposition 1 may be tuned separately given some specified structure of the controller.

Let

$$\Sigma_1:\dot{x}_1=f_1\left(x_1\right),\ f_1:D_1\rightarrow\mathbb{R}^{n-1} \qquad (21)$$

represent the error dynamics of the system (1)-(3) when a control law is applied. Furthermore, let

$$\Sigma_2:\dot{x}_2=f_2\left(x_2\right),\quad f_2:\mathbb{R}\rightarrow\mathbb{R}$$

represent the error dynamics of the observer (6)-(7). Suppose that the control law in Σ_1 uses feedback from the mass flow and that replacing this with the estimated mass flow results in the overall system

$$\Sigma:\dot{x}=f\left(x\right)+g\left(x\right)\quad f:D\rightarrow\mathbb{R}^n \qquad (22)$$

where $x=\left[\begin{array}{cc}x_3^T & x_2\end{array}\right]^T$, $f\left(x\right)=\left[\begin{array}{cc}f_1^T\left(x_3\right) & f_2\left(x_2\right)\end{array}\right]^T$ and $g\left(x\right)=\left[\begin{array}{cc}g_1^T\left(x\right) & 0\end{array}\right]^T$. The function $g\left(x\right)$ results from introducing the estimated mass flow in the control law rather than a measurement. An example on how to arrive at system (22) when introducing the estimated state in an existing control law will be given in Section V-B.

Assumption 3: $V_1\left(x_1\right)$ is a Lyapunov function for the system (21) satisfying

$$\begin{aligned}c_{11}\left\|x_1\right\|^2 &\leq V_1\left(x_1\right)\leq c_{21}\left\|x_1\right\|^2 \quad (23)\\ \dot{V}_1\left(x_1\right) &\leq -c_{31}\left\|x_1\right\|^2 \quad (24)\\ \left\|\frac{\partial V_1\left(x_1\right)}{\partial x_1}\right\| &\leq c_{41}\left\|x_1\right\| \quad (25)\end{aligned}$$

$\forall x_1\in D_1$ for some positive constants $c_{i1}>0$.

Assumption 4:

$$\left\|g_1\left(x\right)\right\|\leq\alpha\left\|x_2\right\|\quad\forall x\in D$$

for some positive constant $\alpha>0$

Proposition 3: Given the systems Σ_1, Σ_2 and Σ as described above. Under Assumption 3 and Assumption 4 the system Σ then has a Lyapunov function $V\left(x\right)$ satisfying

$$\begin{aligned}c_1\left\|x\right\|^2 &\leq V\left(x\right)\leq c_2\left\|x\right\|^2 \quad (26)\\ \dot{V}\left(x\right) &\leq -c_3\left\|x\right\|^2 \quad (27)\end{aligned}$$

$\forall x\in D$. Hence, the system satisfies the conditions for ES on D.

Proof: Let

$$V\left(x\right)=r_1V_1\left(x_3\right)+r_2V_2\left(x_2\right) \qquad (28)$$

where $r_1,r_2>0$. Using (10) and Assumption 3, (28) is upper and lower bounded by

$$\begin{aligned}r_1c_{11}\left\|x_3\right\|^2+\frac{1}{2}r_2x_2^2 &\leq V\left(x\right)\leq r_1c_{21}\left\|x_3\right\|^2+\frac{1}{2}r_2x_2^2\\ c_1\left\|x\right\|^2 &\leq V\left(x\right)\leq c_2\left\|x\right\|^2 \quad (29)\end{aligned}$$

where $c_1=\min\left\{r_1c_{11},\frac{1}{2}r_2\right\}$ and $c_2=\max\left\{r_1c_{21},\frac{1}{2}r_2\right\}$.

TABLE I

a_{01}	$=$	$347[\frac{m}{s}]$
V_p	$=$	$0.03125[m^3]$
A_1	$=$	$0.0414[m^2]$
L_c	$=$	$50[m]$
J	$=$	$60[kgm^2]$
p_{01}	$=$	$10^5\ [Pa]$
σ	$=$	0.9
r_2	$=$	$0.178[m]$

Using Assumption 3, (11) and Assumption 4, the time derivative of (28) along the trajectories of Σ is upper bounded by

$$\begin{aligned}\dot{V}(x) &\leq -r_1 c_{31}\|x_3\|^2 - r_2 k_{\tilde{m}} x_2^2 + r_1 \frac{\partial V_1(x_3)}{\partial x_3} g_1(x) \\ &\leq -r_1 c_{31}\|x_3\|^2 - r_2 k_{\tilde{m}} x_2^2 + r_1 \left\| \frac{\partial V_1(x_3)}{\partial x_3} \right\| \|g_1(x)\| \\ &\leq -r_1 c_{31}\|x_3\|^2 - r_2 k_{\tilde{m}} x_2^2 + r_1 c_{41}\alpha \|x_2\| \|x_2\| \quad (30)\end{aligned}$$

Applying Young's[1] inequality on the term $\|x_1\| \|x_2\|$, an upper bound on (30) is found as

$$\begin{aligned}\dot{V}(x) &\leq -r_1 c_{31}\|x_3\|^2 - r_2 k_{\tilde{m}} x_2^2 \\ &\quad + \frac{\gamma}{2} r_1 c_{41}\alpha \|x_3\|^2 + \frac{1}{2\gamma} r_1 c_{41}\alpha \|x_2\|^2 \quad (31) \\ &= -r_1\left(c_{31} - \frac{\gamma c_{41}\alpha}{2}\right)\|x_3\|^2 \quad (32) \\ &\quad -r_1\left(\frac{r_2}{r_1}k_{\tilde{m}} - \frac{c_{41}\alpha}{2\gamma}\right)\|x_2\|^2 \quad (33) \\ &= -c_3\|x\|^2 \quad (34)\end{aligned}$$

where γ is chosen such that $\left(c_{31} - \frac{\gamma c_{41}\alpha}{2}\right) > 0$, $\frac{r_2}{r_1}$ is chosen such that $\left(\frac{r_2}{r_1}k_{\tilde{m}} - \frac{c_{41}\alpha}{2\gamma}\right) > 0$ and $c_3 = \min\left\{\left(c_{31} - \frac{\gamma}{2}c_{41}\alpha\right), \left(\frac{r_2}{r_1}k_{\tilde{m}} - \frac{1}{2\gamma}c_{41}\alpha\right)\right\} > 0$. From (29) and (34) it can be seen that $V(x)$ is a Lyapunov function for system Σ satisfying the conditions of ES on D. ■

Remark 4: Assumption 1 is no longer needed for the observer due to (21).

V. Simulations

The model used for simulation is the same as used in [9], where the compressor characteristic is approximated with a third order polynomial in both m and ω. The parameters used are given in Table I. The simulation scenario is the same in all of the simulations. The system is initially operating in a open loop stable equilibrium. After 10 seconds the equilibrium point is driven to the left of the surge line by reducing k_t, resulting in an unstable open loop equilibrium point. For the stable equilibrium $k_t = 0.0115$ is used, and for the unstable equilibrium $k_t = 0.0085$ is used. The reduction of throttle opening is simulated by a step in k_t filtered through a first order filter with time constant $T = 1$. The observer gain is set at $k_{\tilde{m}} = 30$.

[1]Young's inequality in a simplified form states that $xy \leq \frac{\varepsilon^p}{p}|x|^p + \frac{1}{q\varepsilon^q}|y|^q$, $\{p, q, \varepsilon\} > 0$, $(p-1)(q-1) = 1$ and $x, y \in \mathbb{R}$

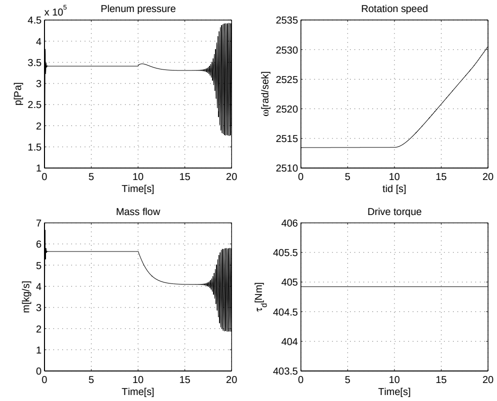

Fig. 2. System states for open loop simulation

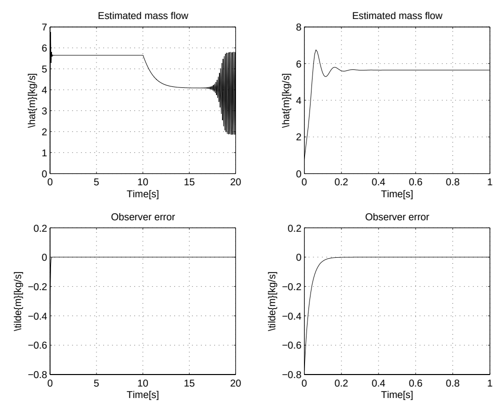

Fig. 3. Observer for open loop simulation

A. Surge

In this simulation it is shown that the model is capable of simulating surge and that the estimated state $\hat{m}$ converges to m. The system (1)-(3) is simulated in open loop with $\tau_d = 400[Nm]$. Fig. 2 shows the system states and Fig. 3 shows the estimate and observer error in the left column and an magnified version of these in the right column. As can be seen from the figures the system enters surge and the observer error converges to zero even when the system experiences surge. This is not surprising since the stability of the observer does not depend on the stability of the state it is estimating.

B. Closed coupled valve control using the estimate $\hat{m}$

In this simulation a closed coupled valve (CCV) control law, [2], is simulated using the estimated state $\hat{m}$ rather than the measured state m. A CCV is a valve immediately downstream of the compressor and its pressure drop is used as a control variable, u. Furthermore, τ_d is used to implement a PI-controller with respect to rotational velocity. The closed loop system is given by

$$\begin{aligned}\dot{\bar{p}} &= \frac{a_{01}^2}{V_p}\left(\bar{m} - \bar{m}_t\left(\bar{p}\right)\right)\\ \dot{\bar{m}} &= \frac{A_1}{L_c}\left(\bar{p}_2\left(\bar{m},\omega\right) - \bar{p} - u\right)\\ \dot{\bar{\omega}} &= \frac{1}{J}\left(\tau_d - \bar{\tau}_c\left(\bar{m},\bar{\omega}\right)\right)\\ \dot{I} &= \bar{\omega}\end{aligned}$$

with the control law

$$\begin{aligned}u &= -k_v\bar{m}\\ \tau_d &= -k_p\bar{\omega} - k_i I - k_d\tanh\left(\frac{m}{\zeta}\right)\end{aligned}$$

and has a Lyapunov function satisfying Assumption 3 on $D_1 = \left\{(\bar{p},\bar{m},\bar{\omega},I) \in \mathbb{R}^4 \middle| p > p_{01} \text{ and } \omega < \omega_{\max}\right\}$ where $\omega_{\max}$ is an arbitrary large constant. In this model

$$\bar{(\cdot)} = (\cdot) - (\cdot)_0 \tag{35}$$

represents the deviation from the equilibrium $(\cdot)_0$. Introducing the estimated mass flow in the control law u it can be seen, by using Definition 1 and (35), that

$$\begin{aligned}u|_{m=\hat{m}} &= -k_v\left(\hat{m} - m_0\right)\\ &= u - k_v\tilde{m}\end{aligned} \tag{36}$$

Introducing the estimated mass flow in the control law τ_d it can be recognized, by using Definition 1, (35) and the mean value theorem, that

$$\begin{aligned}\tau_d|_{m=\hat{m}} &= -k_p\bar{\omega} - k_i I - k_d\tanh\left(\frac{\hat{m}}{\zeta}\right)\\ &= \tau_d + \frac{k_d}{\zeta}\left(1 - \tanh^2\frac{m}{\zeta}\right)\bigg|_{m=z}\tilde{m}\end{aligned} \tag{37}$$

where z is some point on the line segment $L(m,\hat{m})$. Let $\breve{(\cdot)}$ represent the deviation from equilibrium when the estimated mass flow is used in the controller. The closed loop system is then, using (36) and (37), given by

$$\begin{bmatrix}\dot{\breve{p}}\\ \dot{\breve{m}}\\ \dot{\breve{\omega}}\\ \dot{I}\end{bmatrix} = \begin{bmatrix}\frac{a_{01}^2}{V_p}\left(\breve{m} - \breve{m}_t\left(\breve{p}\right)\right)\\ \frac{A_1}{L_c}\left(\breve{p}_2\left(\breve{m},\breve{\omega}\right) - \breve{p} - u\right)\\ \frac{1}{J}\left(\tau_d - \breve{\tau}_c\left(\breve{m},\breve{\omega}\right)\right)\\ \breve{\omega}\end{bmatrix} + \begin{bmatrix}0\\ \frac{A_1}{L_c}k_v\tilde{m}\\ \frac{k_d}{J\zeta}\left(1 - \tanh^2\frac{m}{\zeta}\right)\Big|_{m=z}\tilde{m}\\ 0\end{bmatrix}$$

Since $\left(1 - \tanh^2\frac{m}{\zeta}\right) \leq 1\ \forall m$, it can be recognized that this system can be put in the framework of Proposition 3 with $x_1 = \begin{bmatrix}\breve{m} & \breve{p} & \breve{\omega} & I\end{bmatrix}^T$, $D = \left\{(\breve{p},\breve{m},\breve{\omega},I,\tilde{m}) \in \mathbb{R}^5 \middle| \breve{p} > p_{01} - p_0 \text{ and } \breve{\omega} < \omega_{\max} - \omega_0\right\}$. Hence, the closed loop system using $\hat{m}$ in the feedback control law rather than m is ES. An estimate of the region of attraction will be limited due to the limitation $\breve{p} > p_{01} - p_0$ since $\omega_{\max}$ is a constant that may be chosen arbitrary large.

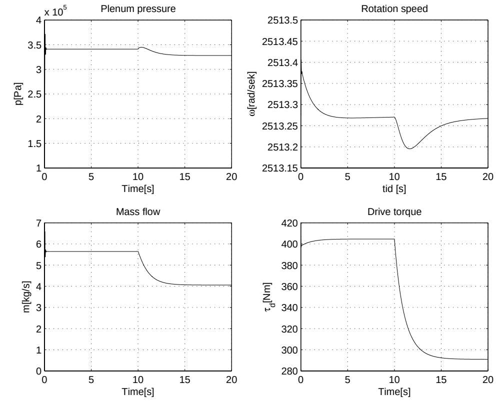

Fig. 4. System states for closed loop simulation

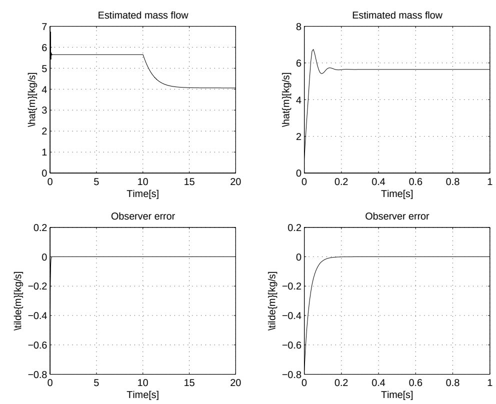

Fig. 5. Observer for closed loop simulation

In simulations the controller gains are chosen as $k_v = 0.2$, $k_p = 60$ and $k_i = 7$. From Fig. 4 and Fig. 5 it can be seen that the controller using $\hat{m}$ renders the open loop unstable equilibrium point stable and that the observer error converges to zero.

VI. Experimental results

In this section the observer from Proposition 2 is tested with experimental data. The data used is from the gas turbine installation in the Energy Technology Laboratory of Eindhoven University of Technology, and is conducted on a compressor without surge control. The test rig is described in [10]. The observer will be applied on two data sets. First the observer is tested on measurements gathered when the compressor is working in a open loop stable operation point, while the other set consist of the compressor experiencing surge. For a more detailed description of the experimental results consult [11].

A. Stable operation

The compressor is initially operating in a equilibrium close to the surge line. After five seconds the throttle valve opening is changed such that the system is driven further into the open

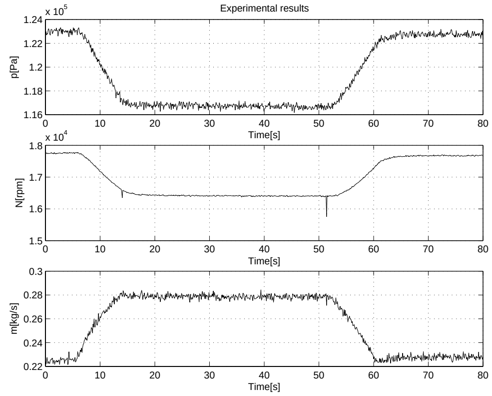

Fig. 6. Experimental data for stable operation

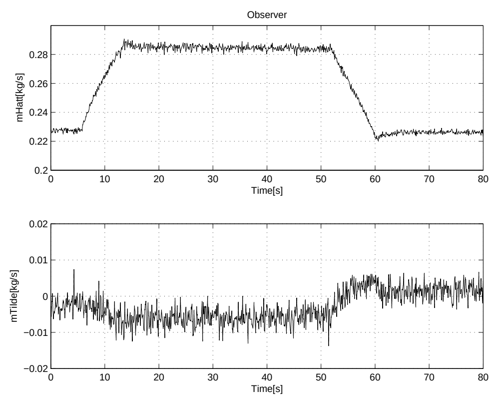

Fig. 7. Observer applied on data from stable operation

loop stable region (away from the surge line) where it settles at its new equilibrium. Then at $t = 52[\mathrm{sec}]$ the throttle opening is changed back to its starting position. Fig. 6 and Fig. 7 show the system states and the observer behavior respectively. From Fig. 7 it can be seen that the observer error varies between approximately -0.007 to 0.002. These deviations counts for 2.5% and 0.9% of the mass flow respectively.

B. Surge

The compressor is initially operating in a stable equilibrium point. After two seconds the operating point is forced over to the open loop unstable operating regime and the system experiences surge. Measurement of the mass flow is absent in the case of surge due to difficulties of measuring transient mass flows. Simulations is therefore used to evaluate the estimated mass flow. The model used for this simulation is described in [11], and the reader is referred to these results for validity of the simulations. Applying the observer from Proposition 2 on the experimental data, results in the estimated mass flow shown in Fig. 8. From Fig. 8 it seems like the estimated state follows the simulations, but a closer inspection of the oscillations showed a deviation in frequency. It can also be seen some deviation in amplitude of the estimated and simulated results.

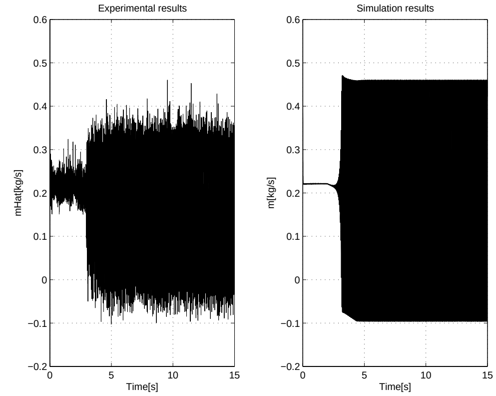

Fig. 8. Observer applied on data from unstabe operation

This is further described in [12].

VII. Conclusion

A GES mass flow observer for compression systems has been presented. A separation principle for the proposed observer has been shown, assuming some property of the control law with respect to feedback from mass flow, allowing the controller and the observer to be tuned separately. The observer was simulated using an existing active surge control law. Further, the observer was tested on experimental data in stable operation and when the system experienced surge.

References

[1] A. H. Epstein, J. E. Ffowcs Williams, and E. M. Greitzer, "Active supression of aerodynamic instabilities in turbomachines," *Journal of Propulsion and Power*, vol. 5, no. 2, pp. 204–211, 1989.

[2] J. T. Gravdahl and O. Egeland, *Compressor surge and rotating stall: modeling and control*, ser. Advances in Industrial Control. Springer-Verlag, 1999.

[3] F. Willems and B. de Jager, "Modeling and control of compressor flow instabilities," *IEEE Control Systems*, pp. 8–18, October 1999.

[4] B. Bøhagen and J. T. Gravdahl, "On active surge control of compressors using a mass flow observer," in *Procedings of the 41th IEEE Conference on Desition and Control*, December 2002.

[5] E. M. Greitzer, "Surge and rotating stall in axial flow compressors, part i: Theoretical compression system model," *Journal of Engineering for Power*, vol. 98, pp. 190–198, 1976.

[6] D. A. Fink, N. A. Cumpsty, and E. M. Greitzer, "Surge dynamics in free-spool centrifugal compressor system," *Journal of Turbomachinery*, vol. 114, pp. 321–332, 1992.

[7] J. T. Gravdahl and O. Egeland, "Centrifugal compressor surge and speed control," *IEEE Transactions on Control Systems Technology*, vol. 7, no. 5, 1999.

[8] H. K. Khalil, *Nonlinear System*, 3rd ed. Prentice-Hall, 2002.

[9] J. T. Gravdahl, O. Egeland, and S. O. Vatland, "Active surge control of centrifugal compressors using drive torque," in *Procedings of the 40th IEEE Conference on Desition and Control*, December 2001.

[10] H. van Essen, "Design of laboratory gas turbine installation," Institute for Continuing Education (IVO), Eindhoven University of Technology, Department of Mechanical Engineering, Section Energy Technology, Tech. Rep. WOC-WET 95.012, March 1995.

[11] J. T. Gravdahl, F. Willems, B. de Jager, and O. Egeland, "Modeling of surge in variable speed centrifugal compressors: Experimental validation," *AIAA Journal of Propulsion and Power*, accepted for publication, 2004.

[12] O. Stene, "Estimering av massestrøm for bruk i aktiv regulering av surge i sentrifugalkompressorer," Master of Science Thesis, Norwegian University of Science and Technology, Department of Engineering Cybernetics, Faculty of Information Technology, Mathematics and Electrical Engineering, June 2003, in Norwegian.